1.3.3 Lab on chip - SAW fluidics

The increasing demand for low-cost and portable devices for biomedical applications has stimulated the development of advanced micro-total-analysis systems (μTAS) [1]. For a full exploitation of the advantages of microfluidics one needs highly controlled liquid flows into biochips. In the common case of hydrophobic capillaries, polar fluids must be forced through microchannels by means of active pumping elements, in order to overcome the large resistance to flow due to the small microchannel sections. The existing pumping systems typically rely on external pressurized lines, which unavoidably limit the portability of microfluidic systems. In the last years, the interaction between surface acoustic waves (SAWs) and liquids was explored as a pumping approach, relying on the streaming effect that drives the fluid flow in the direction of SAW propagation [2]. SAW methods have been mainly limited to mixing, localization or transport of droplets deposited on planar substrates, preferably patterned by regions of different wettability. The main issues of such open digitalized microfluidic architectures are the liquid evaporation and a remarkable sensitivity to surface contamination.
Lab-on-a-Chip research activity at NEST lab aims to the design and realization of handheld, battery-operated chips based on SAW-driven micropumps and closed microchannel networks suitable for automated, high-throughput, cost-effective architectures.

We investigated the application of SAW based pumping methods to microchannel environments fully compatible with μTAS applications, studying the flow of water and protein solutions in prototypical devices made by a piezoelectric $LiNbO_3$ substrate and elastomeric polymer patterns defining the capillary circuits.
We employed a combination of photo- and soft lithography to fabricate devices with different fluidic geometries. The basic layout consisted of two layers. The bottom layer was a $LiNbO_3$ substrate, with two microfabricated interdigital transducers (IDTs) for SAW excitation and detection. The IDTs were composed by 20 pairs of 500-μm-long Al fingers with 24 μm periodicity (~160 MHz resonance frequency on $LiNbO_3$), placed at a distance of 3.4 μm. The upper layer was a patterned polydimethylsiloxane (PDMS) film. Channel geometries with lateral dimensions between 120 and 520 μm and relative heights between 10 and 50 μm were transferred onto PDMS replicas. Final devices were straightforwardly assembled by conformal bonding of the two layers (Fig. 1): the hybrid microchannels were thus defined by the $LiNbO_3$ bottom wall and the PDMS lateral and top walls.

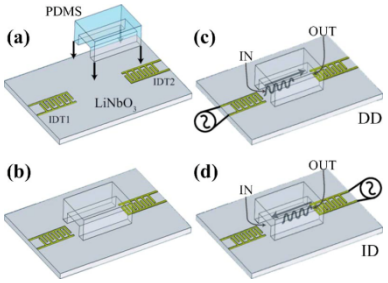

Figure 1. Scheme for the assembling of microfluidic devices and the activation of the liquid motion into microchannels: (a) and (b) final devices were fabricated by the superposition of a PDMS textured element and a $LiNbO_3$ substrate layer with IDTs for SAW excitation and detection; (c) DD and (d) ID experimental arrangements.

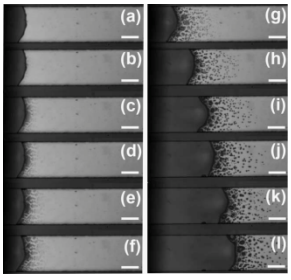

Figure 2. Photographs of the water withdrawing micropumping at different times (t). From (a) to (l): t = 0.00, 0.05, 0.06, 0.08, 0.09, 0.13, 0.53, 1.51, 2.46, 3.48, 4.49, and 5.49 s, respectively. Marker = 100 μm.

The liquid reservoirs consisted in de-ionized water drops of about 2 ml released at the entrance of the microchannels. Continuous SAWs were excited, and the position of the water-air interface within the channel was monitored as a function of time and power of the signal applied to the IDT (P_{SAW}). We analyzed two different experimental arrangements. First, SAWs were excited from one IDT to the channel entrance and, hence, along the channel toward its outlet [direct drive (DD)] [Fig. 1(c)]. Second, the SAWs were launched in the opposite direction, i.e., from the other IDT, so that SAWs propagated from the channel outlet toward its inlet [inverted drive (ID)] [Fig. 1(d)]. In case of conventional DD, with increasing P_{SAW}, we observed droplet deformation caused by acoustic streaming and, finally, a rather slow movement of the liquid into the channel (P_{SAW} = 20 dBm). At these power values, however, significant droplet atomization occurred that strongly affected the droplet outside the channel, where incoming SAW power was maximum. This led to fast evaporation of the water reservoir and prevented the filling of the microchannel.

ID showed a very different behavior [3]. For P_{SAW} >14 dBm, a fast liquid transfer from the reservoir droplet into the microchannel (Fig. 2) was observed. We stress that the liquid was driven in the opposite direction with respect to the SAW propagation direction. In view of the known SAW-fluid interaction properties[2] so far leading to liquid drag only along the SAW direction, this phenomenon was quite unexpected. Figure 2 displays a typical filling process, where water nebulization was visible at the meniscus position. ID pumping is surprising in light of the fact that any momentum transfer to the liquid must be in the opposite direction with respect to actual fluid flow. Conventional acoustic-streaming physics, therefore, does not apply. In order to understand this dramatic difference between the ID and DD behaviors we must consider the different positions where the SAW-liquid interaction occurs. In the ID configuration, the interaction is maximum within the capillary and leads to a drastically enhanced water nebulization rate at the meniscus position. This atomization leads to the formation and growth of water particles sprayed off the main fluid drop within the channel (Fig. 2). The evolution of these droplets and their interaction with the liquid meniscus determine the observed pumping phenomenon: small droplet generation is followed by coalescence and final merging with the meniscus. The latter phenomenon changes the position of the liquid-air interface, resulting in a net fluid movement in the opposite direction with respect to SAW propagation. The filling velocity (v_{fill}) could be controlled up to a maximum value of 1.24 mm/s (i.e., about 0.3 ml /min for the present channel geometry) by varying P_{SAW} up to 20 dBm, yielding rapid filling (t=0.9 s) of the whole channel, without significant evaporation of the droplet reservoir.

We also tested the compatibility of this pumping method with biological solutions [4]. Efficient microchannel filling was easily obtained also for solutions of fluorescent proteins (Fig. 3). For sake of example, in case of a channel with section 200 x 20 μm^2 coupled to an IDT working at a resonance frequency of 151 MHz, a filling velocity of about 50 mm s^{-1} was measured (for W = 21.5 dBm).

Importantly, the protein fluorescence intensity and spectral characteristics (peak wavelength, λ_{E1GFP}, and emission full width at half maximum, $\Delta\lambda_{E1GFP}$ were not

significantly affected by the interaction with the SAW and with the hybrid channel during the entire filling process (Fig. 9). The unaltered protein fluorescence confirms the suitability of SAW withdrawing in microchannels for biological applications.

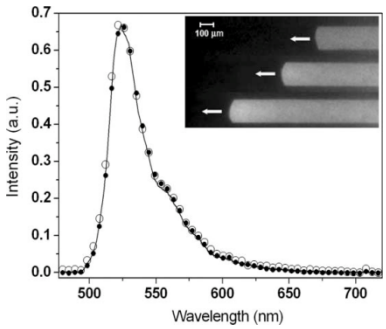

Figure 3. E1GFP emission spectra at the entrance of SAW microchannels (open dots), within microchannels during SAW withdrawing (solid line), and at the exit of the microchannels (full dots). No significant intensity or spectral differences were observed during and after the filling process. For all the spectra, l_{E1GFP} = 524 nm and Dl_{E1GFP} = 29 nm. Inset: fluorescence images of E1GFP solution withdrawing micropumping at different times (t). From top to bottom: t=0.00, 10.15, 19.45 s.

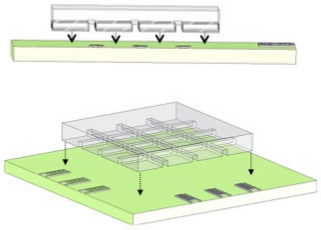

Figure 4. Schematization of a microfluidic chip based on a PDMS microchannel network and IDTs as integrated micropumps.

ID appears to be very promising for the fabrication of integrated micropumps for microfluidic chips and μTAS. Indeed, the present approach requires only an external signal generator set at the IDT resonance frequency. Importantly, impedance matching and device geometry optimization (i.e., channel shape, IDT periodicity/aperture, IDT position, etc.) will enable battery-operated systems.

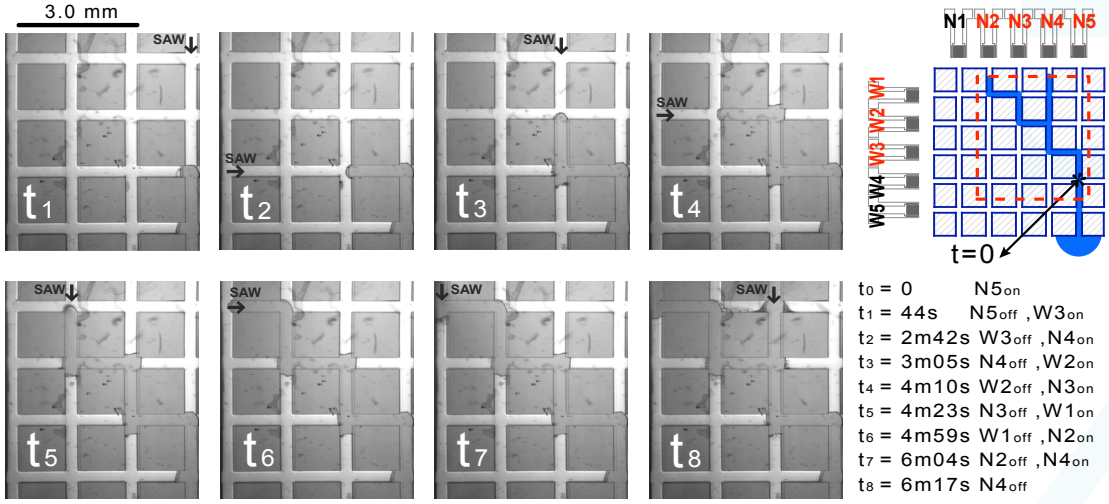

Figure 5. Micropumping cycle exploiting 7 different SAW micropumps acting along a network of 7 microchannels, containing 6 cross areas for a total fluidic volume of 500 nl. The final liquid pattern (t_8) was achieved by inducing 6 direction changes (from t_2 to t_7) and one fluid split (t_8).

Work is in progress to extend this approach to more complex microfluidic networks by integrating several IDTs on the same chip to drive fluids along specific diagnostic paths (Fig. 4). SAW-based counterflow was successfully exploited to control liquids in hydrophobic microchannel arrays. The devices were formed by a 5 × 5 orthogonal array of hybrid $LiNbO_3$/PDMS microchannels (20 input/output ports, 25 crossing areas) and 20 IDTs for SAW excitation and detection. SAW-induced acoustic counterflow was demonstrated capable of: i) filling discontinuous microchannels; ii) inducing 90° flow direction changes; iii) extracting fluid laterally from filled microchannels; and iv) flow splitting and simultaneous multichannel filling. Finally, one example of a complex filling sequence was given showing 6 direction changes and one fluid split (Fig. 5).

Finally, we recently demonstrated a new protocol based on spatiotemporal image correlation spectroscopy to map velocity fields in microfluidic devices[7-8], and automated architectures for on-chip routing of fluids that we believe nicely show the potential for practical implementations based on our pumping mechanism [9].

References

[1] Microfluidics: Fluid physics at the nanoliter scale, Rev. Mod. Phys. **77**, 977 (2005). T M Squires and S R Quake.

[2] Planar chip device for PCR and hybridization with surface acoustic wave pump, Lab. Chip **5** 308 (2005). Z Guttenberg, H Muller, H Habermuller, A Geisbauer, J Pipper, J Felbel, M Kielpinski, J Scriba and A Wixforth

[3] Acoustic-counter-flow micro-fluidics by surface acoustic waves, Appl. Phys. Lett. **92**, 104103 (2008). M. Cecchini, S. Girardo, D. Pisignano, R. Cingolani, and F. Beltram

[4] Polydimethylsiloxane-$LiNbO_3$ surface acoustic wave hybrid micropump devices for fluid control into microchannels, Lab Chip **8**, 1557 (2008). S. Girardo, M. Cecchini, F. Beltram, R. Cingolani, and D. Pisignano

[5] F Beltram, M Cecchini, R Cingolani, S Girardo, D Pisignano "Micro/nanofluidic channels structure fluid motion controlling device for chips (e.g. micromixers) for e.g. biological applications has polydimethylsiloxane structured volume, and piezoelectric substrate having active control mechanism" International Patent WO2009013705-A1 (2007)

[6] Surface-acoustic-wave counterflow micropumps for on-chip liquid motion in two-dimensional microchannel arrays, Lab Chip **10**, 1997 (2010). L. Masini, M. Cecchini, S. Girardo, D. Pisignano, F. Beltram.

[7] Easy monitoring of velocity fields in microfluidic devices using spatiotemporal image correlation spectroscopy, Anal Chem **85**, 8080 (2013). M. Travagliati, S. Girardo, D. Pisignano, F. Beltram, and M. Cecchini.

[8] Fabrication, operation and flow visualization in surface-acoustic-wave-driven acoustic-counterflow microfluidics, JoVE **78**, e50524 (2013). M. Travagliati, R. Shilton, F. Beltram, and M. Cecchini.

[9] Interaction-free, automatic, on-chip fluid routing by surface acoustic waves, Lab chip **12**, 2621 (2012). M. Travagliati, G. De Simoni, C. M. Lazzarini, V. Piazza, F. Beltram, M. Cecchini.